AFRC 2024 Industrial Combustion Symposium
Calgary, Alberta, Canada
September 30 – October 3, 2024

Swiss-roll Combustor: A Compact Portable Solution for Addressing the Methane Emissions from Low-production Oil and Gas Sites

Authors: Patryk Radyjowski[1], Erika Lieberknecht[1], Daksh Adhikari[1,2], Parthib Rao[1], Chien-Hua Chen[1], Patharapong Bhuripanyo[3] and Paul Ronney[3]

[1] Advanced Cooling Technologies, Inc., Lancaster, PA, USA
[2] Georgia Institute of Technology, Atlanta, GA, USA
[3] University of Southern California, Los Angeles, CA, USA

1. Introduction

Methane (CH_4) is a powerful greenhouse gas with a global warming potential at least 27 times that of CO_2 over a 100-year span. Reductions in CH_4 atmospheric release have significant potential to address the extreme temperature increase, thus alleviating the harmful effects of climate change [1]. The oil and gas (O&G) industry accounts for a substantial share of the total methane emissions [2], second only to aerobic fermentation. Within the O&G sector, flaring devices are typically used to mitigate methane and other VOC emissions. While there is a strong push for zero routine flaring by 2030, flaring remains the most economically and technically feasible solution for many small emission sources. As of 2017, there were roughly 97,000 flares in Texas, with about a third burning less than 20 MSCFD and about half with less than 50 MSCFD [3]. Due to the large quantity of these small emission sources, the methane destruction efficiency of such flaring systems greatly impacts the methane emissions. The existing small-capacity open flares (<100 MCF/day) suffer from uncertain methane destruction efficiency due to susceptibility to environmental factors such as wind and are generally less efficient when operating at lower capacity. While enclosed combustors mitigate the environmental factors issue, they are typically large and bulky and therefore not suitable for small and portable applications. Moreover, most of the flares operate in non-premixed combustion mode, which generates high NO_x and soot emissions. Consequently, there is a distinct need for a compact, clean combustion system that is able to achieve near 100% destruction efficiency over a wide range of gas stream composition and flow rates while minimizing NO_x and other emissions (e.g., soot, $PM_{2.5}$). The Swiss-roll combustor (SRC) is one such technology that has the potential to address these needs.

Swiss-roll Combustor Technology

The heat-recirculating combustor concept, proposed by Weinberg [4], provides a highly efficient method for efficiently combusting a wide range of fuels. The Swiss-roll is one of the most compact designs, which includes a combustion chamber surrounded by a spiral heat exchanger, shown schematically in Figure 1A. Weinberg's original design has fuel and air injected from the inlet. However, a fluctuation of the flare gas flow rate can result in a strong mixture transiently present in the inlet channel and, therefore, the flashback or auto-ignition risk. To avoid such a possibility, the new design introduces fuel near the combustion zone, where there is sufficient mixing time but an insufficient auto-ignition time. As shown in Figure 1A, the air flow mixes with fuel near the center and enters the reaction zone, where the combustion occurs, while the hot products flow out from the core through the adjacent outlet channel. The heat transfer from the hotter outlet channel to the cooler inlet channel through the spiral heat exchanger significantly increases the incoming reactants' temperature, thus combustion temperature and reaction rates. Figure 1B further illustrates the temperature increase resulting from heat recirculation. The resulting reaction temperature can be higher than the adiabatic flame temperature, called the "super-adiabatic" flame temperature. This extends the flammable range of various fuels and promotes the achievement of equilibrium state concentrations, hence high destruction efficiency. Due to the large reaction zone area in the center of the Swiss-roll compared to a propagating flame, the combustion inside the Swiss-roll can be sustained at a temperature

lower than typical combustion, reducing NO_x formation significantly. Previous experiments using a sub-scale Swiss-roll (1 ft x 1 ft) showed between 0-1 ppm NO_x emission [5].

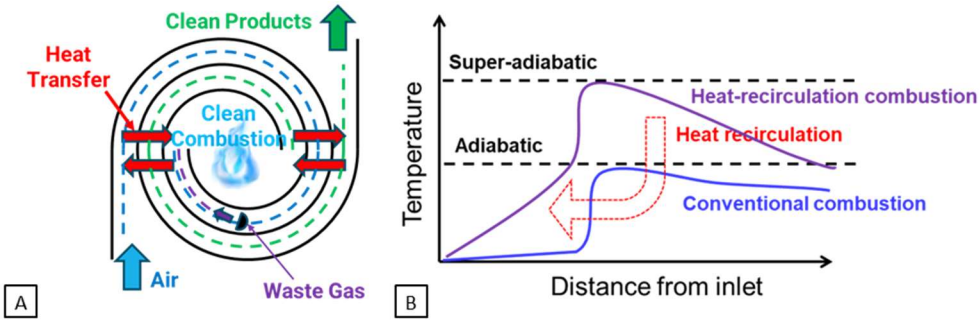

Figure 1: The Swiss-roll Combustor (A) Principle of operation showing main flows and heat transfer path, (B) Influence of heat recuperation on combustion temperatures leading to super-adiabatic conditions in the core that promote complete combustion.

2. High-Temperature Ceramometallic Swiss-roll Combustors

Prior work on Swiss-roll devices concentrated on small-scale units used to examine the principle and study physical principles of operation. Limited work investigated an all-metal 12" Swiss-roll for residual Volatile Organic Compound (VOC) incineration [5]. Although showing excellent destruction efficiency, the thin metal structure severely limited the core temperature and suffered thermal deformation. The novel Siliconized Silicon Carbide (Si-SiC) utilizing Additive Manufacturing (AM) methods addresses those issues by providing high-temperature ceramometallic materials that can be formed in complex shapes required by Swiss-roll geometry. Simultaneous implementation of a new material system with scale-up of base SRC design into size sufficient for high MSCFD-scale flare operation has been performed. The resulting 9" experimental Swiss-roll geometry with 1.75 turns and central fuel injection has been manufactured in-house in Si-SiC, instrumented, and test-fired over various flaring conditions. The effort has been supplemented with a detailed 2D Computational Fluid Dynamics (CFD) simulation to reproduce the experimental measurements and use it as a modeling tool for future development.

Experimental Setup

The Si-SiC 9" SRC core has been manufactured at Advanced Cooling Technologies (ACT) using a multi-step process including binderjet 3D printing, vacuum pyrolyzation, and Si metal infiltration. Figure 2C shows the details of the experimental SRC core geometry. The resulting core unit, shown in Figure 2A, can operate with surface temperatures up to 1350°C while retaining sufficient strength to maintain structural integrity. Notably, this unit has been created with the top wall purposefully absent. Instead, a more traditional solution, a machinable ceramic plate with metal backing, has been used to allow for the instrumentation of the experimental apparatus. Custom metal manifolds handle the inlet and outlet connections to the Si-SiC core, while fuel is supplied from the top via a narrow pipe with equispaced small holes, as shown in Figure 2B.

The external support system diagram is shown in Figure 3. Air and gases are supplied by dedicated mass flow controllers (MFC). This configuration allowed strict control over the combustible mixture and enabled the production of both heavily N_2 diluted and high BTU/SCF simulated flare gas streams. The ignition is provided by a hot wire inserted into the core via the top plate. A bank of pressure transducers measured pressure drop through the system core. Multiple K- and R-type thermocouples were used to record temperatures in positions indicated by Figure 2C. The CH_4 destruction removal efficiency (DRE) measurement was based on gas chromatograph (GC) measurement of the exhaust stream under steady conditions and the MFC setting of incoming fuels. The SRI 8610GC allowed for 50ppm CH_4 resolution translating to sub-% DRE measurement resolution with exact accuracy depending on flow conditions. Finally, a Testo 350 Flue Gas Analyzer has been used to record the exhaust's O_2, CO, NO, and NO_2 levels.

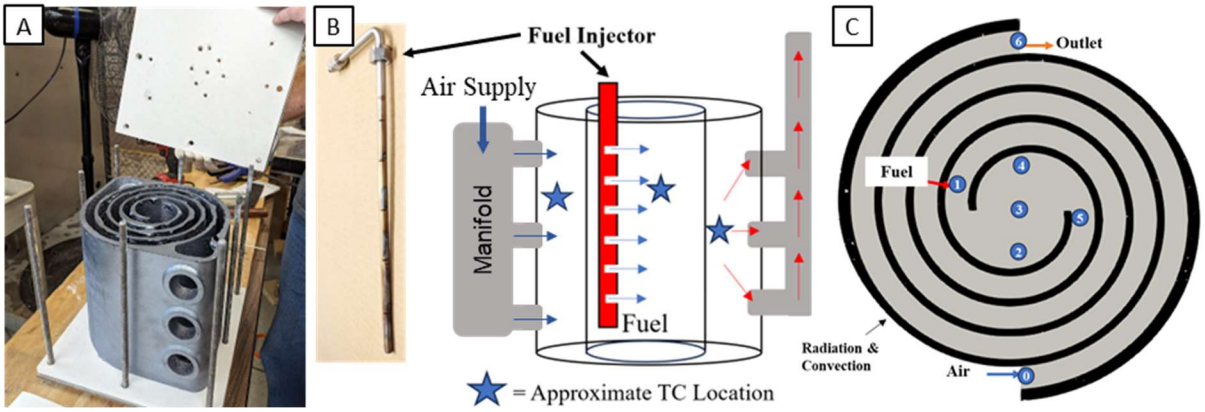

Figure 2: The 9" Swiss-roll combustor experimental unit (A) Partially assembled view, (B) Flow schematic for the system, (C) Top view indicating thermocouples positions.

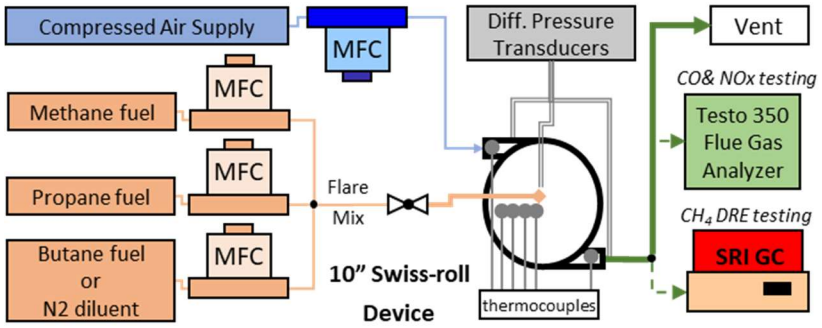

Figure 3: Schematic of the experimental apparatus.

The complete system is shown in Figure 4A. The SRC experiments executed with smooth ignitions and minimal operator input required. Figure 4B shows the system with no visible flame under full thermal power operation.

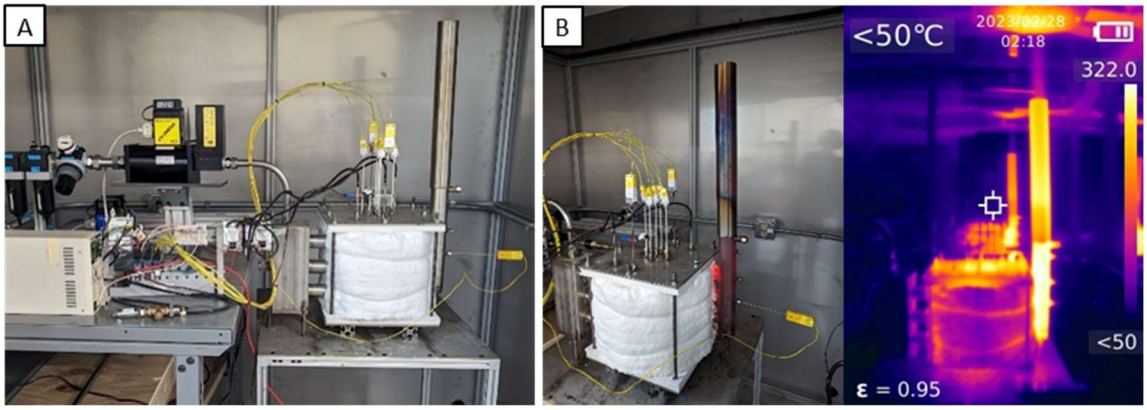

Figure 4: The experimental apparatus overview (A) and during operation (B).

Experimental Results

The steady-state operation map at a range of equivalence ratios Φ and total flow rates through the SRC is shown for methane operation in Figure 5A. The green square overlay shows the conditions where 99%+ DRE has been recorded. CH_4 combustion is shown as the most challenging hydrocarbon to destroy in a flaring device completely. Experimental SRC shows a wide range of operating point with steady running at as low as Φ = 0.15 (566% excess air) and up to 3.6 MSCFD fuel flow, with nearly all measured points showing 99%+ methane DRE. The high thermal mass and strong gas-solid thermal coupling also allow the

unit to operate at abnormal conditions without DRE efficiency loss. This was demonstrated by a single test, where a steady condition of Φ = 0.25 was followed by known too-lean Φ = 0.125. The combustor started to cool down, but the combustion maintained a key 99%+ DRE even after 2 minutes.

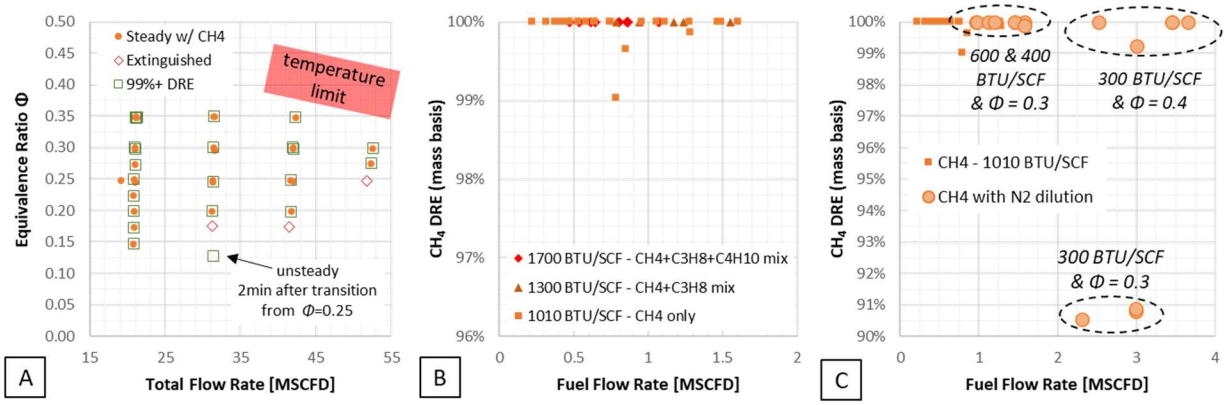

Figure 5: 9" SRC experimental results: (A) stability map, (B) CH_4 DRE for high BTU/SCF cases, (C) CH_4 DRE for low BTU/SCF cases.

The SRC's DRE performance has also been investigated with a range of fuel mixtures:

- High BTU/SCF, where a mixture of CH_4, C_3H_8, and C_4H_{10} were used to meet 1350 and 1700 BTU/SCF. The steady-state operation was confirmed over the 0.5 to 1.2 $MSCFD_{mix}$ range and $0.25 \leq \Phi \leq 0.4$. The SRC was able to operate steadily, and temperatures remained within the material limits. The DRE measurements for high BTU/SCF cases, shown in Figure 5B, never dropped below 99.8%.
- Low BTU/SCF, where CH_4 fuel was diluted with inert nitrogen. The 600, 400, and 300 BTU/SCF values were investigated at Φ = 0.3. All cases reached a steady operation, but the DRE measurement, Figure 5C, showed that Φ = 0.3 is too lean (too cold) to destroy the methane entirely, hence lower DRE. Increasing Φ to 0.4 resolved this issue entirely.

A summary of recorded pressure drop data between the SRC core and outlet over a range of fuel flow rates is shown in Figure 6A. The experimental unit measured between 0.5 and 1 inH_2O pressure drop at 1 $MSCFD_{fuel}$ with higher pressure drop at leaner conditions due to a higher overall flow rate. The log-log plotting allows to predict that more than 30 $MSCFD_{fuel}$ is achievable below 10 inH_2O pressure drop. Hence, flow obstruction is not a limiting factor for high flow rate operations, at least for the 9" prototype.

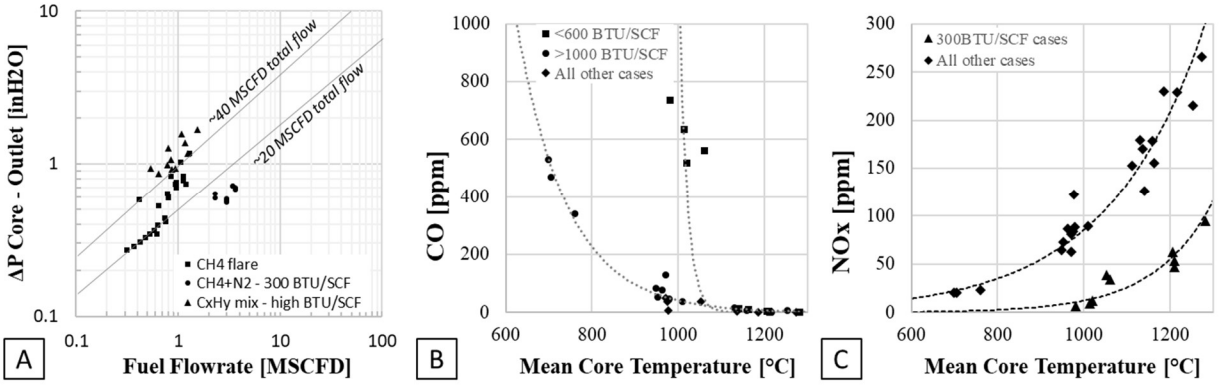

Figure 6: 9" SRC experimental results: (A) pressure drop vs. fuel flow rate, (B) exhaust CO levels vs. mean core temperature, and (C) exhaust NO_x level vs. meant core temperature. All plots combine data from all steady-state measurements.

The CO and NO_x emissions at mean core temperatures are plotted in Figures 6B and 6C, respectively. The experimental SRC showed very low CO production rates, usually below 100 ppm for most cases. Only the marginal cases at extremes of flammability limits and energy content (300 BTU/SCF and 1700 BTU/SCF) registered increased CO production, usually accompanied by decreased DRE. Meanwhile, substantial amounts of NO_x were detected even at lower mean core temperatures, which indicated poor fuel mixing with diffusion flame jets stretching from the injection pipe. Notably, the increased momentum of 300BTU/SCF, due to all additional N_2 diluent, provided adequate mixing to partially-premixed operation, hence reduction in NO_x. The identified fuel mixing issue is being addressed in future SRC designs.

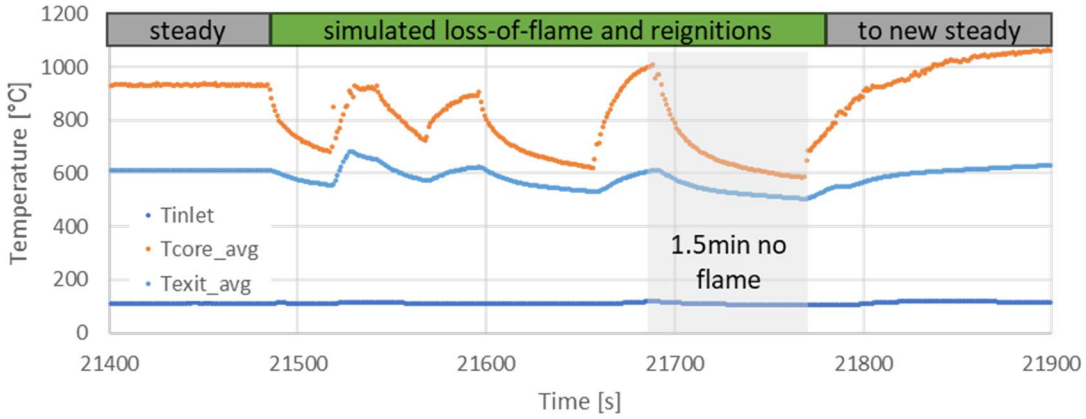

Figure 7: Swiss-roll reignition example based on repeated simulated loss of flame (fuel disabled) followed by auto-ignition.

The high thermal mass of SRC allows for seamless reignition once the flare mixture returns to flammable conditions, a unique capability beneficial for flaring applications. The temperature record on an auto-ignition test, where a loss of flame was simulated by completely stopping the fuel gas flow, is shown in Figure 7. The 9" SRC showed excellent reignition performance, where temperatures started to rise immediately upon the re-introduction of fuel. The longest tested period of "flame lost" was 1.5 minutes, followed by the seamless reignition, despite the mean core temperature dropping below 600°C.

The experimental SRC has successfully operated for a total of 56 hours over 12 cooldown heat-up cycles. SRC core temperatures usually remained between 1000-1200°C but reached as high as 1300°C in some instances. The picture of the core wall, the hottest part of SRC, before and after the experiments is shown in Figure 8. The loss of metallic shine is due to a thin SiO_2-SiC passivation layer forming that protects the underlying material. This is a good prognosis for Si-SiC longevity in flare incineration applications, however further long-term durability testing is required.

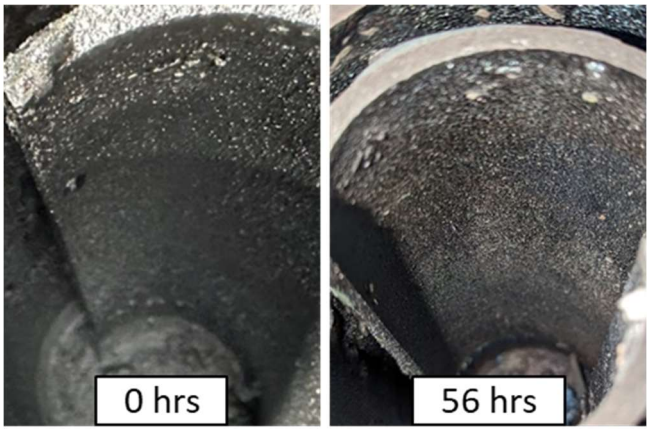

Figure 8: View of the SRC core wall (hottest element) before and after 56 hours of combustion experiments.

CFD Model Setup

Computational Fluid Mechanics (CFD) is a valuable tool for enhancing knowledge of thermo-mechanical flow systems. Recently, computers have become powerful enough to model complex combustion problems, including those of Swiss roll combustors. A dedicated CFD model has been developed to simulate the experimental SCR geometry and compare it with the measured values reported previously.

The 2D model of the experimental SRC combustor was created and solved using OpenFOAM version 7 [6]. A RANS k-omega turbulence model was implemented, and a no-slip boundary condition was utilized for the walls. The partially stirred reactor turbulent combustion model, PaSR, from OpenFOAM, was used for the combustion model with a reduced GRI-Mech 3.0 [7] model for methane combustion (36 species and 217 reactions), where nitrogen chemistry was removed to speed up computations. CFD model also includes a P1 Radiation model with an ambient temperature of 300K and the Marshak Radiation boundary condition with a constant emissivity value of 0.8 for solid walls. The out-of-plane volumetric heat sink's thermal resistance model, shown in Figure 9C, assumes a 1cm ceramic insulation block and 0.5 mm aluminum support structure to mimic a typical experimental configuration. The conductive heat transfer coefficient was specified using equation (1) based on conditions specified by Cramer et al [8]. The fluid domain was transient and solved using the PIMPLE, PISO (Pressure-Implicit Split-Operator)-SIMPLE (Semi-Implicit Method for Pressure-Linked Equation) method. The solid domain was solved in a steady state to allow the model to finish in a time-efficient manner. Therefore, the SIMPLE method was used. Two cases, shown in Table 1, are discussed in more detail, but a total of 25 simulations were performed.

Table 1: Inlet conditions for detailed CFD analysis

Flow rate at STP [SLPM]	**Actual flow rate at inlet conditions [LPM]**	**Equivalence Ratio Φ [-]**
400	600	0.325
400	600	0.35

Figure 9A shows the overall computational mesh with 144,526 cells. The following Figure 9B shows a zoomed-in section of the 2D mesh near the outlet. The average cell size through the channel is 1.36 mm.

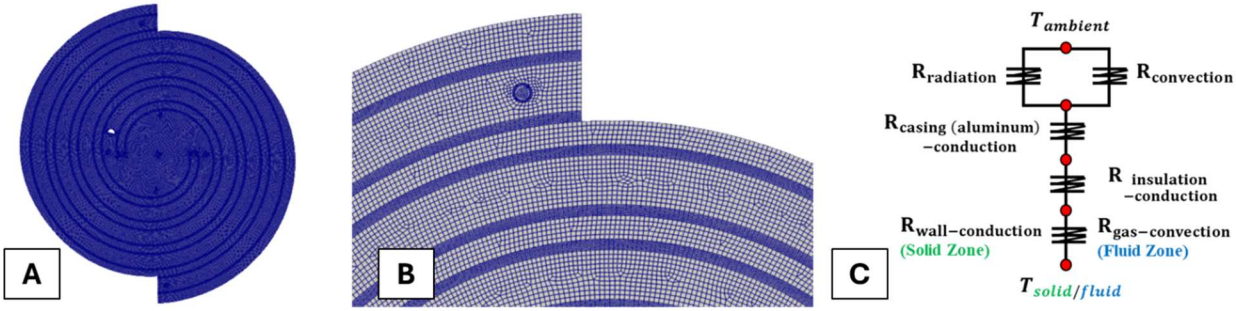

Figure 9: 2D computational mesh: (A) Full view, (B) Zoomed-in at the outlet (C) Depiction of the out-of-plane thermal model used as volumetric sink.

Figure 2B illustrates the conceptual design of the computational domain. The black area is the solid domain, and the beige is the fluid domain, with arrows indicating the flow direction. Locations of interest are numbered (0)-(6) and correspond to thermocouple placements used in the experimental setup:

Air Inlet (0): Air enters through the inlet at the figure's bottom. The channel width is 15mm, and the inlet air temperature was set to 400K. The ambient pressure was set to 1E5 Pa. The boundary condition is set as velocity inlet, with velocity varied depending on the case shown in Table 1. The inlet species are 21% O_2 and 79% N_2.

Fuel Injector/inlet (1): Fuel inlet width is 5.5 mm. The fuel is comprised of pure methane at 300K. A velocity boundary condition is also used here. The fuel velocity was varied based on the desired equivalence ratio Φ, the deviation of the actual air-to-fuel ratio from the stoichiometric ratio.

Combustion Chamber (2-4): The combustion chamber is positioned centrally and is surrounded by the spiral heat exchanger. Point 3 specifies the location of the artificial ignition source used in the numerical model.

Combustion Exit (5): This is an area of interest because the flow velocity increases as it exits the combustion chamber, moving towards the outlet, and CH_4 slip can be tracked.

Outlet (6): Hot combustion products exit through the outlet at the figure's top. This setup was used to model a forced flow system, hence a velocity boundary condition was utilized instead of setting a pressure gradient condition. The temperature specified at the outlet was 300K.

Computational Results

The purpose of the SRC is to limit the ppm, parts per million, of the fuel methane, CH_4, after combustion to less than 50 ppm. Therefore, Figure 10 shows the CH_4 contour across the domain on a logarithmic scale stretching from 100% CH_4 down to 1ppm level.

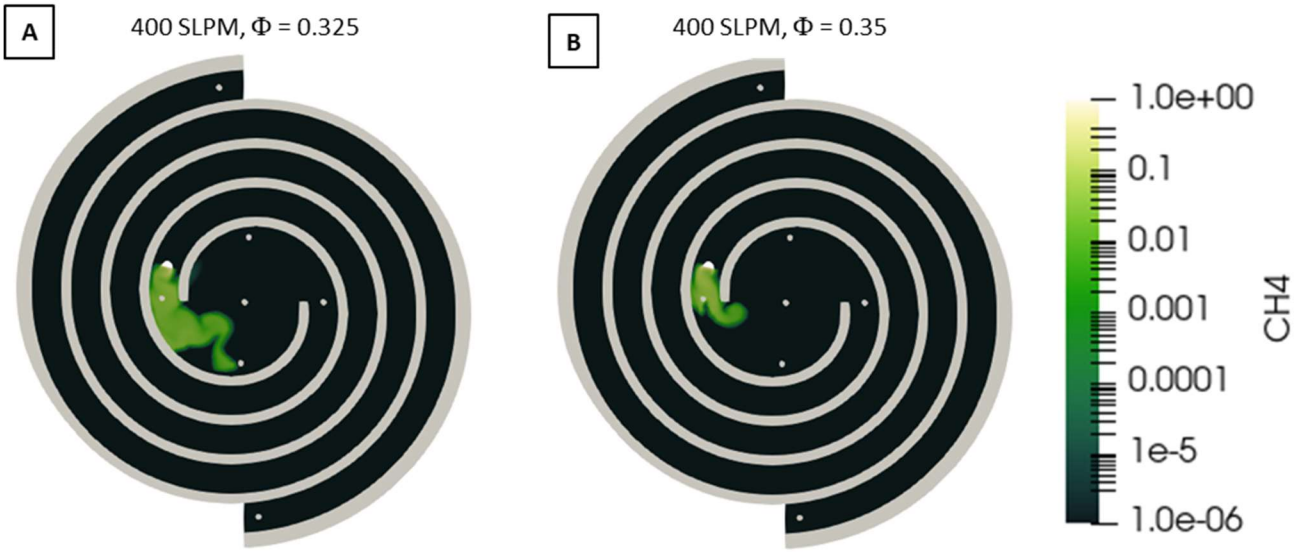

Figure 10: Methane mass fraction contour: (A) 400 SLPM, Φ =0.325, (B) 400 SLPM, Φ=0.35

In Figure 10, the value 1.0E-6 is equivalent to one ppm. This output evaluates the efficiency of the SRC for methane combustion. In shown results and all investigated steady cases, there were no 1+ ppm_{CH4} levels past the SRC core.

A series of temperature contour plots for the 400 SLPM, 0.325 Φ case is shown in Figure 11. The contour plot highlights the temperature distribution across the domain, offering insights into temperature gradients and ranges. Notably, the flow exiting the combustion chamber is distinctly hotter than the flow entering the domain. This will result in a non-uniform thermal stress distribution across the structure.

The computational predictions were evaluated against the experimental measurements, and the results are summarized in Figure 12. The comparison revealed a 15% or less percent error except for point (1), SRC inlet, for the Φ = 0.35 case. A potential source of discrepancy at this location is the near presence of a highly variable flame front and the vertical (out of simulation plane) effects. This shows the limitations where the vertical averaging of 2D simulation fails to reproduce the relative fuel port to thermocouple tip arrangement, as shown in Figure 2B. The percentage error decreases after combustion, points three through six, providing further confidence in the combustion model and resulting temperature load profiles.

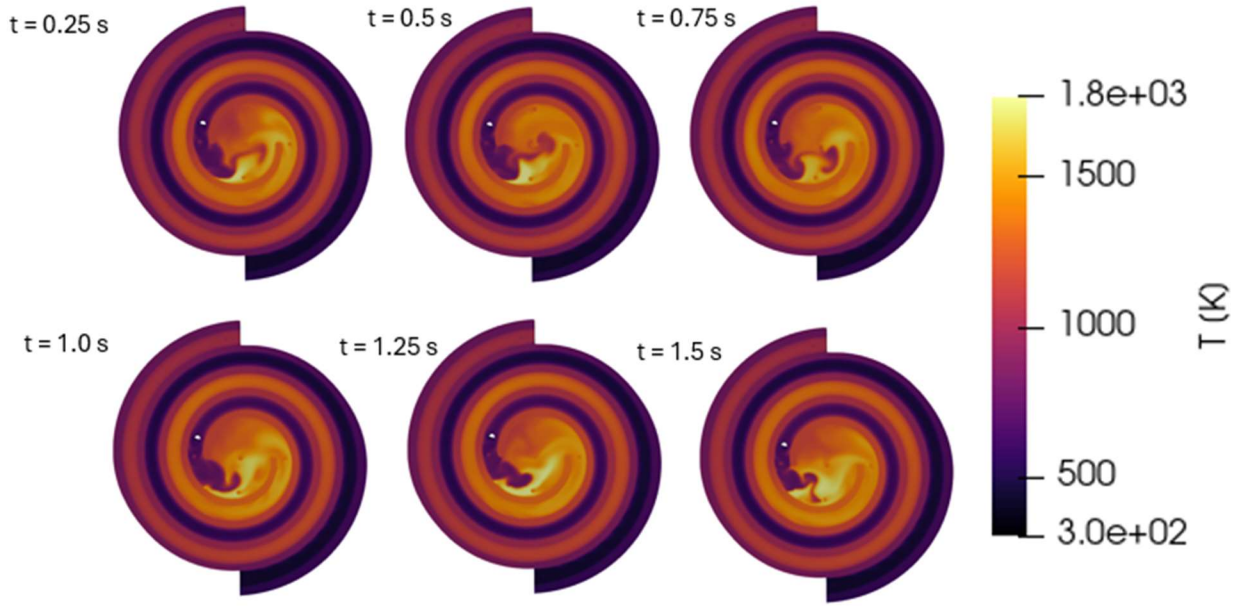

Figure 11: The temperature contour plot for the case 400 SLPM, Φ = 0.325 at various time intervals.

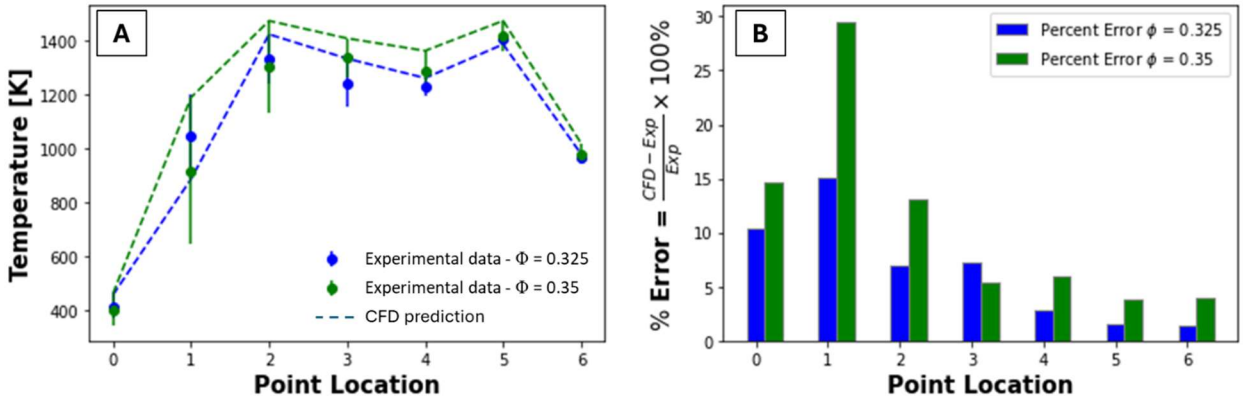

Figure 12: The 400 SLPM$_{flow}$ experimental data were compared with the computational results. (A) Thermocouple [points] and CFD output [dash line], (B) Percent error

3. SRC Designs for Small Emission Source Applications

The experimental combustor proved the potential for Swiss-roll devices to address small flaring needs at 99.5%+ methane destruction efficiency over a wide range of conditions. This section discusses current work towards practical SRC systems to address ground-level needs at O&G sites. Figure 13 shows an example of Swiss-roll implementation as a continuous emissions control device at a small oil drilling and processing facility. The device is especially suitable for operations where vapor recovery or gas utilization is economically or practically unsustainable. In such cases, an efficient combustion is the only method to address the associated gas production from oil sites. Thanks to the wide operating range, the SRC can accommodate any mixture of the primary gas from the phase separator (low BTU/SCF) and the secondary off-gas from storage tanks (high BTU/SCF). Further optimizations, such as integrated self-fueled flame pilots, are possible in future deployments.

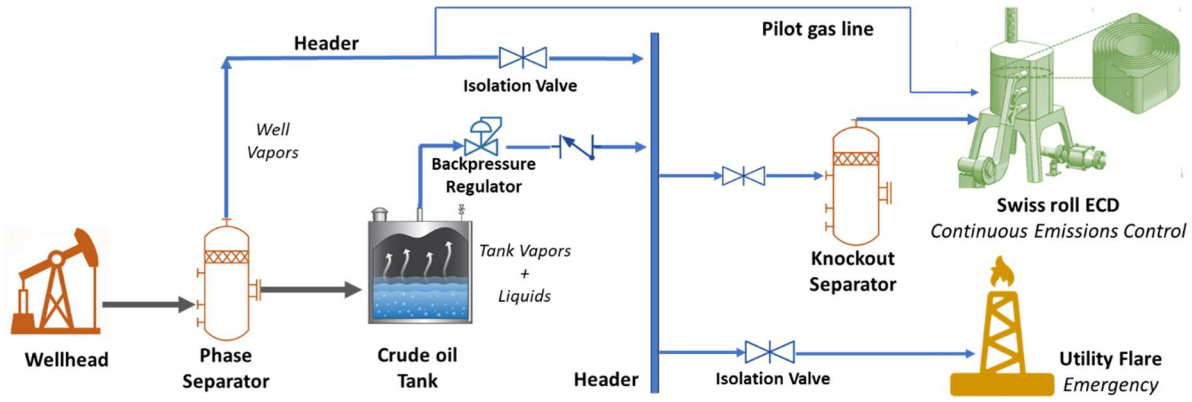

Figure 13: Potential SRC implementation on small wellhead and gas processing site for continuous emissions control.

Passive Flow Configuration for Cost-Oriented Applications

The small size of potential applications puts strong constraints on operating costs and the complexity of flaring systems. Therefore, an entirely passive system without the blower is of particular interest. The natural draft created by a dedicated stack can generate a pressure differential to aspire a sufficient amount of air for stable operation at lower fuel flow rates. The 12" passive SRC structure, Figure 14A, has been optimized for low flow resistance by widening the flow channel, reducing the number of turns, and increasing combustion zone size. Those changes reduced the system pressure drop below 0.5 inH_2O. The CFD model also included a fully resolved 15-foot vertical stack at the exit with a prescribed pressure differential, hence buoyancy forces drive all flow. The CH_4 and temperature contours at 2 MSCFD fuel inlet, Figures 14B and 14C, respectively, show a steady operation with complete methane destruction. It has been found that passive system stability is greatly improved by including a small pilot flame, equivalent to 0.06 $MSCFD_{C3H8}$, at the entrance to the combustion core. A small pilot also allows the unit to maintain the exhaust temperature where no primary flaring gas is available.

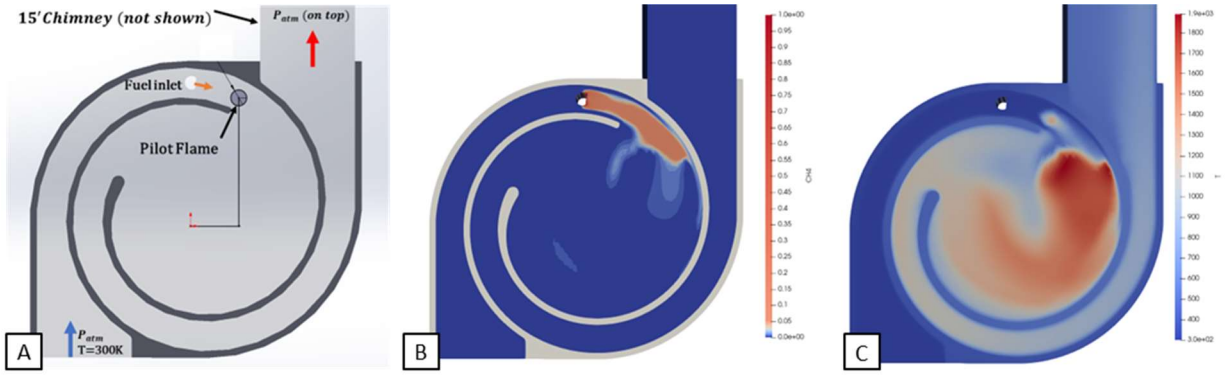

Figure 14: 12" SRC design for passive operation: (A) general geometry, (B) CH_4 mass fraction, and (C) temperature contours for a naturally aspired operation at 2 MSCFD fuel input with a small pilot flame.

The follow-up CFD study investigated the system response to sudden changes in waste gas flow rate, Figure 15A, for the system with and without an active pilot. Brief fluctuations between 1 and 4 MSCFD were studied after 20 seconds of steady operation. Furthermore, the nitrogen chemistry has been added back to the combustion mechanism to examine the NO_x production. The SRC successfully maintained the flame even at the highest fuel fluctuations and quickly returned to base operating mode afterward. The detailed CO and NO_x emissions at stack exhaust are shown in Figures 15B and 15C for cases without and with active pilot, respectively. It should be noted that emissions reading is delayed with respect to the original flow disturbance due to the substantial propagation distance to reach the top of the chimney.

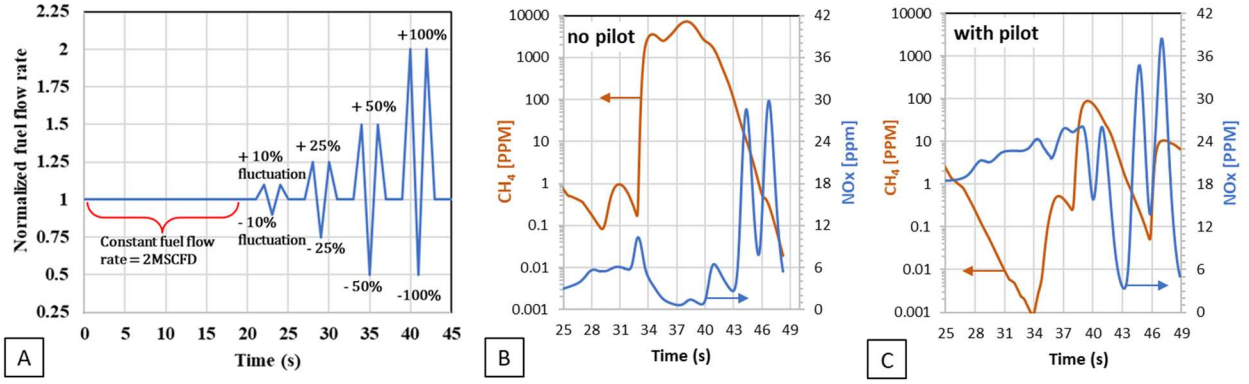

Figure 15: CFD flow variability analysis for passive SRC: (A) studied profile, (B) CO & NO_x emissions without pilot, (C) CO & NO_x emissions with active pilot

The pilot-less operation results in lower base NO_x and acceptable <1 ppm CH_4 under steady conditions. However, even a ±50% fuel fluctuation severely disrupts the flame, allowing major CH_4 to escape into the atmosphere combined with NO_x peaks as the system reignites. In contrast, the active pilot simulation benefits from improved stability of well-anchored flame and never emits more than 100ppm of CH_4, maintaining 99%+ DRE. Nonetheless, this comes at the cost of increased NO_x emissions from pilot flame. The work continues to further the understanding of SRC dynamics and optimize the design.

This numerical study found that steady operation in a passive mode with high CH_4 DRE is possible for properly designed SRC combustors. The draft-driven system is also self-regulating, dramatically reducing the control system's complexity. This is a desirable solution for small O&G operations requiring continuous emissions control.

Forced Flow Configuration for High-Performance Applications

Compactness, modularity, and high throughput (flow rate) with no visible flames are most important for flaring operations located in densely populated areas or as a part of scheduled maintenance. For such applications, the forced flow SRC configuration with a 12" Si-SiC core is of interest. Figure 16 shows an example of a CAD design of such a system with deployment-ready metal packaging for a Swiss-roll core. The entire flare gas and air handling, including a 1.5 hp blower, is contained within a 6' x 3' footprint. The SRC core is interfaced with the supply system via a dedicated steel casing, where a spring-loaded construction allows for differential thermal expansion. A similar system design is being constructed, and field testing is planned in the near future.

Active control over the air stream allows for precise adjustment of flame conditions for DRE optimization and thermal regulation, which enables significantly higher flare gas flow rates. The core design features an extended inlet section to provide improved fuel-air mixing. Nonetheless, the substantially higher flow rates require flow path streamlining to maintain manageable pressure drop, hence the similarity with a passive design. The pressure field for 230 $MSCFD_{air}$ is shown in Figure 17A, where an acceptable 3.5 inH_2O overall pressure drop is predicted. Figure 17B shows the CFD results for related 10 MSCFD CH_4 flare flow cases with the equivalence ratio of $\Phi = 0.75$ (left) and $\Phi = 0.7$ (right). Both cases have an elongated flame interface thanks to high flow momentum. The slower flame speed of the leaner mixture ($\Phi = 0.7$) results in the CH_4 contour periodically reaching the core outlet, hence allowing a small methane slip. This has not been observed in a richer flow case, which indicates the importance of correct air-to-fuel ratio control in maintaining high methane destruction in this application.

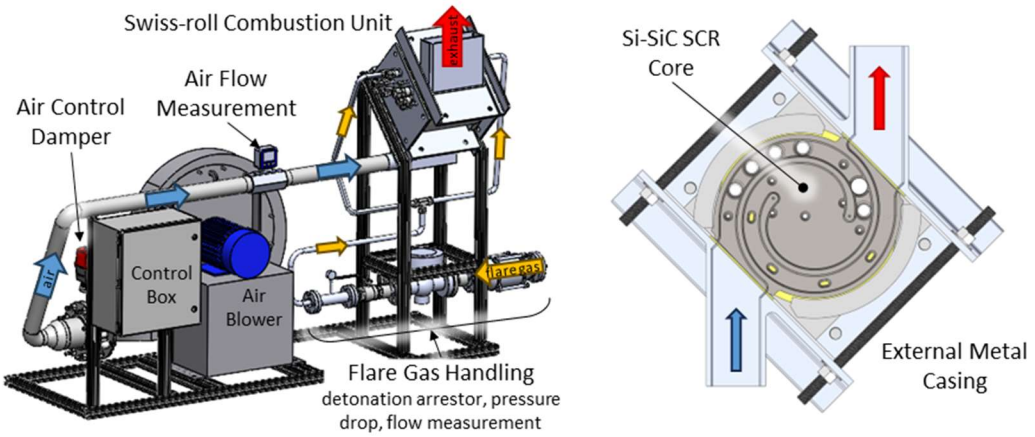

Figure 16: Early CAD concept of compact 12" SRC forced flow system for high-performance applications

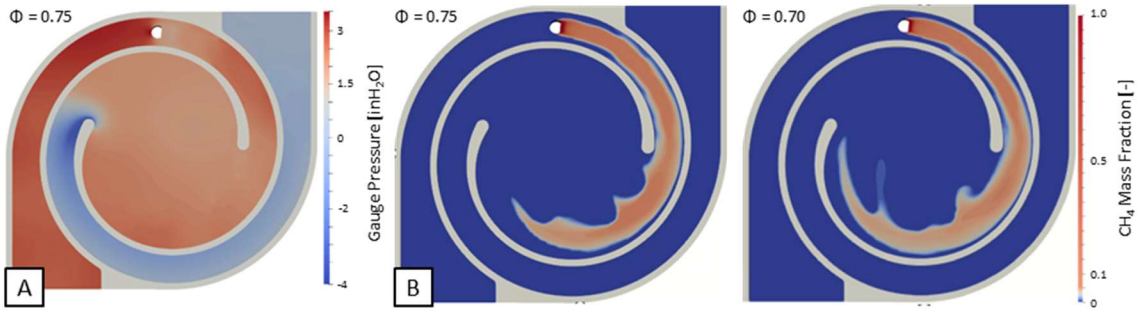

Figure 17: CFD simulation for 12" SRC forced flow system: (A) gauge pressure contour for 230 $MSCFD_{air}$ air & 10 $MSCFD_{CH4}$; ΔP_{total} ~3.5 inH_2O and ΔP_{fuel} ~0.9 inH_2O, (B) CH_4 mass fraction at 10 $MSCFD_{CH4}$ inlet at Φ=0.75 & Φ=0.7

4. Conclusion

The paper discusses recent developments in a promising Swiss-roll flaring technology that offers 99%+ methane destruction efficiency in a compact and conditions-flexible package. The combination of thermally efficient design with novel ceramometallic Si-SiC material enables super-adiabatic combustion, hence faster chemistry, addressing the concerns of short residence time. The experimental 9" SRC has been manufactured and tested at ACT. The experiments showed a wide operating range with various fuels, including heavily N_2-diluted natural gas (300 BTU/SCF) and energy-rich heavier hydrocarbon mixtures (up to 1700 BTU/SCF). The 100% CH_4 destruction efficiency has been recorded for nearly all cases. Pressure drop and emissions data have been obtained for further analysis and design improvements. Furthermore, the unique ability of igniter-free restart after 90 seconds of no fuel flow has been demonstrated. The structure inspection after 56 hours of operation showed no oxidation damage to the material. A detailed 2D CFD model has been developed in OpenFOAM solver, including k-ω turbulence, detailed chemistry (GRI-Mech 3.0), and P1 radiation model. The simulation results show good temperature agreement with experimental data. The developed CFD simulation is a valuable tool in the qualitative analysis of new SRC system designs. Firstly, the blower-free passive systems are particularly interesting for small oil pumping operations. A CFD simulation of an optimized SRC core shows a stable 2 $MSCFD_{CH4}$ operation with a natural draft provided by a 15' stack. The CFD study shows that SRC has good resiliency to major fuel flow fluctuation up to +100%/-50% while maintaining high DRE when the pilot flame is involved. Meanwhile, a blower-operated system shows promise for sustained high throughput operations. A field demonstration of such a system is currently being prepared.

5. Acknowledgments

This research was funded by the Advanced Research Projects Agency-Energy (ARPA-E) under contract number DE-AR0001538. The authors thank the program manager Dr. Jack Lewnard for his support during the project.

6. References

[1] P. A. Arias *et al.*, "Climate Change 2021 – The Physical Science Basis Working Group I Contribution to the Sixth Assessment Report of the Intergovernmental Panel on Climate Change," in *Climate Change 2021 – The Physical Science Basis*, Cambridge University Press, 2023, pp. 35–144. doi: 10.1017/9781009157896.002.

[2] EPA, "Inventory of U.S. Greenhouse Gas Emissions and Sinks: 1990-2022 U.S. Environmental Protection Agency, EPA 430R-24004.," 2024. https://www.epa.gov/ghgemissions/inventory-us-greenhouse-gas-emissions-and-sinks-1990-2022

[3] R. Sitton, "Sitton Texas Flaring Report Q1 2020," 2020. [Online]. Available: https://www.rrc.texas.gov/media/vhhj43cq/sitton-texas-flaring-report-q1-2020.pdf

[4] S. A. Lloyd and F. J. Weinberg, "A burner for mixtures of very low heat content," *Nature*, vol. 251, no. 5470, pp. 47–49, Sep. 1974, doi: 10.1038/251047a0.

[5] J. Crawmer, C.-H. Chen, B. Richard, H. Pearlman, T. Edwards, and P. D. Ronney, "An Innovative Volatile Organic Compound Incinerator," in *36th International Conference on Thermal Treatment Technologies & Hazardous Waste Combustors*, 2018, pp. IT3-22.

[6] H. G. Weller, G. Tabor, H. Jasak, and C. Fureby, "A tensorial approach to computational continuum mechanics using object-oriented techniques," *Comput. Phys.*, vol. 12, no. 6, pp. 620–631, Nov. 1998, doi: 10.1063/1.168744.

[7] G. P. Smith *et al.*, "GRI-Mech 3.0," 2023. http://www.me.berkeley.edu/gri_mech/

[8] C. L. Cramer *et al.*, "Properties of SiC-Si made via binder jet 3D printing of SiC powder, carbon addition, and silicon melt infiltration," *J. Am. Ceram. Soc.*, vol. 104, no. 11, pp. 5467–5478, 2021, doi: 10.1111/jace.17933.